SEARCH FOR POLARIZATION EFFECTS IN THE ANTIPROTON PRODUCTION PROCESS

D. Grzonka, K. Kilian, J. Ritman, T. Sefzick

Institut für Kernphysik, Forschungszentrum Jülich, 52425 Jülich, Germany

W. Oelert

Johannes Gutenberg-Universität Mainz, 55099 Mainz, Germany

M. Diermaier, E. Widmann, J. Zmeskal

Stefan-Meyer-Institut für subatomare Physik, 1090 Wien, Austria

B. Głowacz, P. Moskal, M. Zieliński

Institute of Physics, Jagiellonian University, 30-348 Kraków, Poland

M. Wolke

Department of Physics and Astronomy, Uppsala University, 75120 Uppsala, Sweden

P. Nadel-Turonski

Thomas Jefferson National Accelerator Facility, Newport News, Virginia 23606, USA

M. Carmignotto, T. Horn

Physics Department, The Catholic University of America, Washington, DC 20064, USA

H. Mkrtchyan, A. Asaturyan, A. Mkrtchyan, V. Tadevosyan S. Zhamkochyan

A.I. Alikhanyan Science Laboratory, Yerevan 0036, Armenia

S. Malbrunot-Ettenauer

CERN, Physics Department, 1211 Genve 23, Switzerland

W. Eyrich, F. Hauenstein, A. Zink

Institut, Universität Erlangen, 91058 Erlangen, Germany

For the production of a polarized antiproton beam, various methods have been suggested including the possibility that antiprotons may be produced polarized which will be checked experimentally. The polarization of antiprotons produced under typical conditions for antiproton beam preparation will be measured at the CERN/PS. If the production process creates some polarization, a polarized antiproton beam could be prepared by a rather simple modification of the antiproton beam facility. The detection setup and the expected experimental conditions are described.

1. Introduction

Polarization observables reveal more precise information of the structure of hadrons and their interaction, and the disentangling of various reaction mechanisms is often only possible by controlling the spin degrees of freedom. With beam and target particles both being polarized quantum states can be selectively populated. For example, in $\bar{p}$–p reactions, a parallel spin configuration of antiproton and proton ($\bar{p}\uparrow \ \ p\uparrow$) is a pure spin triplet state and with an antiparallel spin configuration ($\bar{p}\uparrow \ \ p\downarrow$) the spin singlet state is dominant. The possibility of adjusting different spin configurations is important for various topics in the regime of high as well as low energy.

While polarized proton beams and targets are routinely prepared, the possibilities for the preparation of a polarized antiproton beam are still under discussion. Proposals for the generation of a polarized antiproton beam have already been presented before the first cooled antiproton beams were available. Methods that have been discussed are: hyperon decay, spin filtering, spin-flip processes, stochastic techniques, dynamic nuclear polarization, spontaneous synchrotron radiation, induced synchrotron radiation, interaction with polarized photons, Stern–Gerlach effect, channeling, polarization of trapped antiprotons, antihydrogen atoms, and also a possible polarization of produced antiprotons. Summaries of the various possibilities can be found in [1–4]. Most of the methods are not usable due to the extremely low expected numbers of polarized antiprotons or the low degree of polarization, and for some methods reasonable calculations are not possible since relevant parameters are not known. Due to the large required effort, no feasibility studies have been performed so far.

A well known source for polarized antiprotons is the decay of $\bar{\Lambda}$ into $\bar{p}\,\pi^{+}$ with a $\bar{p}$ helicity of 64.2 ($\pm$ 1.3)% (the more precise value for Λ decay is taken) in the $\bar{\Lambda}$ rest frame [5]. By measuring the direction and momenta of the $\bar{\Lambda}$, the $\bar{p}$, and π^{+} in the laboratory system, the decay kinematics can be reconstructed and the transversal and longitudinal antiproton polarization components in the lab system for each event can be determined.

The method was used at FERMILAB in the only experiment with polarized antiprotons so far [6] studying the polarization dependence of inclusive $\pi^{\pm}\pi^0$ production. A proton beam of 800 GeV/c momentum produced antihyperons $(\bar{\Lambda})$ and their decay antiprotons with momenta around 200 GeV/c. A mean polarization of 0.45 was observed but the polarized antiprotons do not constitute a well defined beam and at lower energies the situation further deteriorates. For the preparation of a pencil beam of polarized antiprotons, other methods are required.

Presently, the most popular proposal is the filter method on a stored antiproton beam, by which one spin component is depleted due to the spin dependent hadronic interaction of a beam passing a polarized target. The filter method in a storage ring was first suggested 1968 in order to polarize high energy protons in the CERN ISR [7]. For filtering of antiprotons at lower momenta it was later pointed out that the new technique of phase space cooling is mandatory and the relevant parameters were shown [8, 9]. In 1993, a feasibility study of the filter method with phase space cooling was performed with a proton beam on polarized protons at the TSR in Heidelberg showing clearly the buildup of polarization [10]. A polarization of about 2% was achieved after 90 minutes filtering time. For antiprotons, the filter method with cooling should also work if one can find any filter interaction with both large spin–spin dependence and cross section. Till now, there are no data for the spin–spin dependence of the total $\bar{p}p$ cross section. From theoretical predictions, one expects that longitudinal polarization effects are larger than transversal effects [11–14]. The consequence might be that a Siberian snake is needed in the filter synchrotron. Experimental $\bar{p}p$ scattering data are needed to work out the conditions and expected properties of a polarized $\bar{p}$ beam prepared by the filter method. The PAX Collaboration is working on this topic with polarized protons as filter [12, 15, 16]. The spin filter method has been demonstrated at COSY for transverse polarized protons and similar studies for longitudinal polarization are planned [17]. Another filter reaction with large polarization effect, which was recently proposed [18], is the interaction with polarized photons but the low intensity of available photon beams together with the small cross section makes it unlikely to produce sufficient polarized antiprotons for significant experiments.

A simple possibility for a polarized antiproton beam may be the production process itself. If the antiproton production process creates some polarization it would be rather simple to prepare a polarized antiproton beam [19].

2. Search for polarization in antiprotons production

It is well known that particles, like *e.g.* Λ-hyperons, produced in collisions of high energy unpolarized protons show a significant degree of polarization [20]. Maybe also antiprotons are produced with some polarization but, up to now, no experimental studies have been performed in this direction.

The production of antiprotons is typically done by bombarding a solid target with high momentum protons. At CERN, the beam momentum is about 24 GeV/c and the number of collected antiprotons is of the order of one per 10^6 beam protons. The production mechanism seems to be a rather simple quasi-free p–nucleon interaction. The $\bar{p}$ momentum spectrum, which is peaked around 3.5 GeV/c, is consistent with a pure phase space distribution for a four particle final state: $pp \to pp\bar{p}p$. The basic process is a creation of baryon–antibaryon out of collisional energy. If transverse polarization occurs (Fig. 1), then a polarized beam can be prepared in a rather simple and cheap way by blocking up and down events, and one side of the angular distribution. Furthermore, the pure S-wave region around 0 degree (< 50 mrad) has to be removed. A simple modification of the extraction beam line of an existing $\bar{p}$ production and cooler facility with absorbers would be sufficient to extract a polarized beam. Of course, one has to avoid polarization loss in de-polarizing resonances in the accumulator cooler synchrotron. This has to be taken into account when such a facility will be constructed. But, first of all, it has to be investigated whether the production process creates some significant polarization.
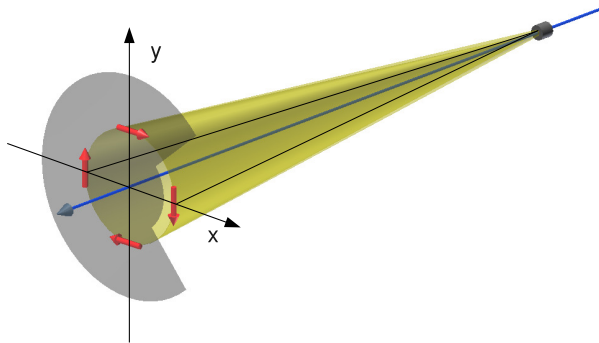

Fig. 1. Possible polarization vector for a given production polar angle θ, indicated by the dark grey/red arrows. In order to select an antiproton beam with transverse polarization, one spin direction has to be separated by a suitably shaped absorber plate as indicated in grey.

3. Asymmetry measurement of produced antiprotons

In view of a future polarized antiproton beam, the polarization studies will be performed at the typical conditions for antiproton beam preparation. Actually, the only facility for antiproton beams is the AD at CERN where the antiprotons, produced with the 24 GeV/c PS proton beam, are injected at a momentum of 3.5 GeV/c. Similar conditions are foreseen for the future FAIR facility.

In order to measure the polarization of the produced antiprotons, a scattering process with known and sufficiently high analyzing power has to be performed.

Well known and calculable is the analyzing power in the high energy pp elastic scattering in the Coulomb nuclear interference (CNI) region. The analyzing power in the CNI region at high energies is attributed to the inference between a non-spin-flip nuclear amplitude and an electromagnetic spin-flip amplitude [21–23, 25]. The maximum analyzing power is approximately given by [21, 24]: $A_N^{\max} = \sqrt{3}/4\,\sqrt{t_p}/m\,(\mu - 1)/2$, with μ = magnetic moment, m = mass. A maximum of 4–5% is reached and the four-momentum transfer at the peak $t_{\rm p}$ is given by: $t_{\rm p} = -8\pi\sqrt{3}\alpha/\sigma_{\rm tot}$, with the fine-structure constant α and the total cross section $\sigma_{\rm tot}$, which results in a value of $t_{\rm p} \sim -3 \times 10^{-3}$ (GeV/c)^2 assuming a total cross section of 40 mb. Experimentally, a maximum analyzing power of about 4.5% at $t = -0.0037$ GeV/c was achieved which is shown in the lower part of Fig. 2. The data are from [25] taken with a 100 GeV/c proton beam at a polarized atomic hydrogen gas jet target.

For antiprotons, the same analyzing power will result because at these energies, the hadronic part is limited to the non-spin-flip amplitude in the CNI region and the spin-flip Coulomb amplitude which changes the sign. This was also experimentally verified in a measurement at FERMILAB with 185 GeV/c polarized antiprotons [26] resulting in an analyzing power of $-4.6\,(\pm 1.86)$%. At 3.5 GeV/c momentum, the assumptions for high energy may not be valid any more. The total elastic cross sections for pp and $\bar{p}p$ at 3.5 GeV/c differ strongly which may indicate a stronger influence of additional amplitudes and could result in a strong deviation from the high energy value of the analyzing power. Also the total cross section of $\bar{p}p$ scattering is about a factor of 2 higher than compared to the 40 mb at high energy which also indicates a shift of the CNI region to lower values. Preliminary calculations of the analyzing power at lower beam momenta have been performed by Haidenbauer [27] in a one boson exchange model with the NN potential adjusted to experimental data of $\bar{p}p$ scattering [28] which are available down to about 5 GeV/c. The maximum in the analyzing power for the calculations for 5 GeV/c $\bar{p}$ momentum is at a t-value of about
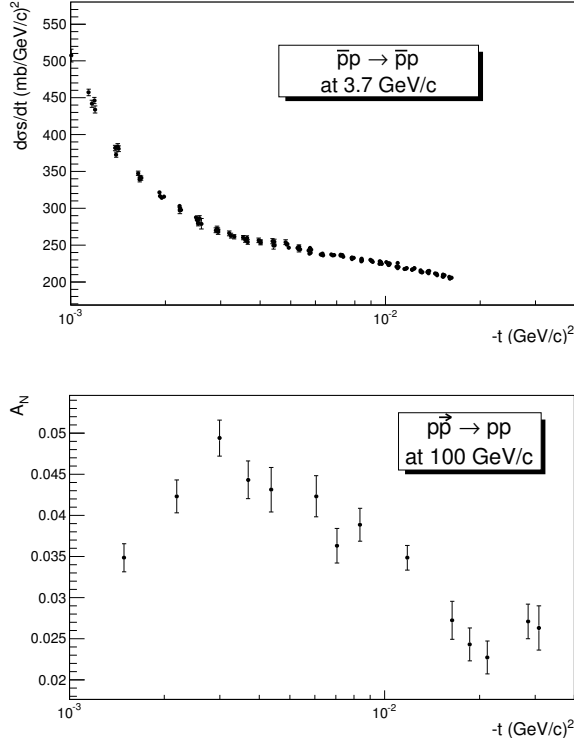
Fig. 2. Cross section data for elastic antiproton–proton scattering at a beam momentum of 3.7 GeV/c [33] (upper part) and analyzing power of proton–proton scattering [25] (lower part) as a function of the four momentum transfer t. The data for the analyzing power have been taken with a proton beam momentum of 100 GeV/c at a polarized atomic hydrogen target. The analyzing power of antiproton scattering is of the same size with opposite sign.

-0.0025 which is a bit lower than the t_{p} value at high energies but the maximum $A_N^{\max}$ is still about 0.45%. Therefore, we expect for a 3.5 GeV/c antiproton scattered on a proton an analyzing power comparable to the high energy data of about 4.5% at a laboratory scattering angle between 10 to 20 mrad.

In Fig. 3 the setup for the proposed polarization study at the T11 beam line of the CERN PS complex is shown.

The T11 beam line delivers secondary particles produced by the 24 GeV/c momentum proton beam of the CERN/PS at a production angle of about 150 mrad with an acceptance of $\pm$ 3 mrad horizontally and $\pm$ 10 mrad vertically [29]. The beam line can be adjusted to momenta of up to 3.5 GeV/c for positively and negatively charged particles. For positively charged particles
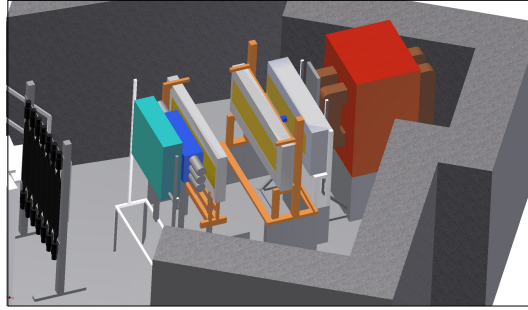
Fig. 3. T11 area with installed detector components. On the right-hand side, the last dipole of the beam line is seen from where the beam enters the detector system.

of momenta of 3.5 GeV/c with open collimators, the momentum resolution is $\pm 5\%$ and up to 1×10^6 particles/spill are delivered with a setting for positively charged particles. The incident proton beam flux at this conditions is between 2×10^{11} and 3×10^{11} and the spill length is 400 ms.

From measurements at comparable conditions [30] (antiproton momentum 4 GeV/c, production angle 127 mrad), a total flux of negatively charged particles of about 5×10^5/spill is expected which include about 4000 $\bar{p}$.

The detector arrangement for the measurement is shown in Fig. 4. It consists of scintillators for trigger signal generation and beam profile measurements, a drift chamber stack to measure the track of the produced an-
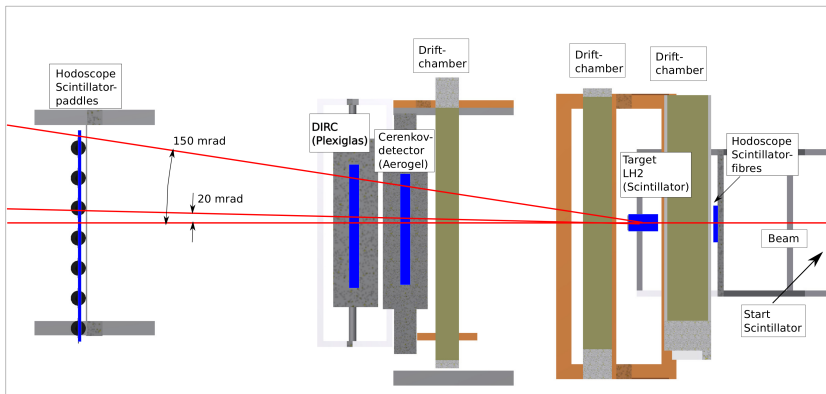

Fig. 4. Sectional drawing of the detector arrangement in the horizontal plane. The beam is entering from the right and hits start scintillator, beam hodoscope, first drift chamber, scattering target, drift chamber pair, Cherenkov detector, DIRC, and scintillator hodoscope. A detailed description is given in the text. The relevant scattering angle for the asymmetry measurement of 20 mrad is indicated by the black/red line. In total, a scattering angular range of about 150 mrad is covered by the system. A similar angular range is covered in vertical direction.

tiproton, an analyzer target, a second drift chamber set to reconstruct the track of a scattered antiproton, a Cherenkov detector for pion discrimination, a DIRC for offline particle identification, and another scintillator hodoscope for trigger and $\bar{p}/\pi^-$ distinction by the time of flight. At the exit of the beam line tube, which ends in front of the last beam line dipole, a scintillation detector is mounted which will be used as a start detector for the timing and trigger generation. A scintillation fibre hodoscope follows which will be used to determine the beam profile. The drift chambers foreseen for these studies have been used in the COSY-11 experiments at the cooler synchrotron COSY in Jülich [31]. The first chamber D1 has a hexagonal drift cell structure, optimized for low magnetic field sensitivity, with 3 straight and 4 inclined (± 10 deg.) wire planes [32]. The drift chamber set for the measurement of scattered antiprotons include 4 (2) straight and 4 (4) inclined (± 10 deg.) planes for D2 (D3). A track resolution of the order of 1 mrad was achieved with 1 GeV/c protons for D1 and the D2, D3 set.

As analyzer target, a liquid hydrogen cell with a length of 15 cm will be used. The reconstructed tracks of primary and scattered antiproton allow to determine the reaction vertex with some uncertainty due to the limited track precision. For the analysis, only the central part will be taken into account in order to discriminate reactions from the target windows. As alternative, an analyzer target consisting of several layers of 4 mm thick scintillators is foreseen. The carbon nuclei from the scintillator material will introduce a rather high background level but the scintillators can act as trigger for elastic $\bar{p}p$ scattering events in the relevant forward angular range. An antiproton passing a scintillator will result in a minimum ionizing energy loss signal. In the case of an elastic $\bar{p}p$ scattering process, an additional energy loss from the scattered proton will be seen. In figure 5, the energy losses as a function of the t-value in plastic scintillators of 4 mm and 10 mm thickness are shown for Monte Carlo data of 3.5 GeV/c $\bar{p}p$ and $\bar{p}C$ scattering in addition to the expected energy loss of a minimum ionizing particle. In the relevant t-range around $t = -0.0037$ GeV/c^2, a clear separation of $\bar{p}p$ events is visible but quasi elastic processes like $\bar{p}C \rightarrow \bar{p}pX$ are not included in the MC data and will give rise to additional background signals. About 20 layers of scintillator modules are foreseen which result in a thickness comparable to the liquid hydrogen target.

The whole system will be operated in the air. The straggling in the material between the first drift chamber and exit window of the beam tube does not influence the measurement. The straggling in the material of the detection system is below the expected track resolution of the drift chambers. For 3.5 GeV/c momentum antiprotons, the radiation length up to the target including D1 and the flight path of ~ 0.5 m in the air is about 30 g/cm^2 with a mean thickness of 0.13 g/cm^2 which introduces a straggling of about
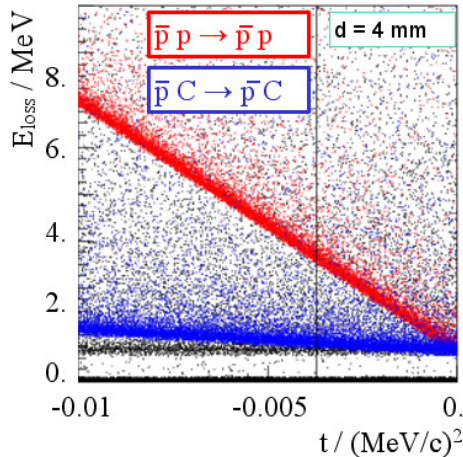
Fig. 5. Simulation of the energy loss in plastic scintillators of 4 mm thickness for 3.5 GeV/c antiprotons passing the scintillator without reaction (black dots), elastically scattered on a carbon nucleus (light grey/blue dots) or elastically scattered on a proton (grey/red dots) in the relevant t-range.

0.2 mrad. The tracking system for the scattered antiprotons gives a straggling of below 0.8 mrad and the hydrogen target adds another 0.7 mrad straggling. With a 10 cm CH target, the straggling will be increased to 2 mrad, which would still be low enough to measure the region of scattering angles around 20 mrad.

At the exit of the tracking system, an aerogel Cherenkov detector ($n \sim 1.03$) to discriminate the expected high pion background will be installed. The Cherenkov signals will be included in the trigger as veto. When the event selection is reduced to single tracks at small scattering angles, most background channels are suppressed and the momenta of the scattered particles are close to the momenta of the primary particles. Antiprotons with 3.5 GeV/c momentum have a velocity of $\beta_{\bar{p}}$ (3.5 GeV/c) = 0.966 , *i.e.* the threshold for Cherenkov light emission is at $n = 1.035$. For pions, which will be the main background source, the velocity is close to c (β_{π}(3.5 GeV/c) = 0.9992) with a threshold refractive index of $n = 1.0008$. Therefore, a threshold Cherenkov detector with $n \sim 1.03$ will drastically suppress the expected large pion background.

Behind the Cherenkov counter, a DIRC with Plexiglas as radiator [34] is mounted for offline particle identification. The separation between antiprotons and pions at 3.5 GeV/c is expected to be 7.8σ deduced from recently performed test measurement with a proton beam at COSY. And finally, a scintillator hodoscope to trigger on single track events is positioned at a distance of about 6.8 m from the start scintillaor. It consists of scintillator paddles with a width of 10 cm readout on both ends by photomultipliers.

With the expected rate of up to 10^6 particles/s at the T11 beam line, a trigger signal has to be generated which selects antiproton scattering events while discriminating the background particles which are mostly pions. An online track reconstruction to be used as event trigger would be very difficult with this event rates. For a trigger signal, we request a signal in the start scintillator and a signal in the scintillator hodoscope at the end and, in addition, a signal from the threshold Cherenkov detector as veto. With this condition, only charged particles which pass through the whole detector arrangement are detected, and if the particle is a pion or a faster one it creates Cherenkov light with a high probability and blocks the trigger signal output. From calculations and test measurements, a pion discrimination by a factor 40 is expected which brings the event rate down to 25 000 events/s for the spill length of 400 ms which is sufficiently low that it can be stored by the data acquisition system without losses. The extraction of elastic scattering events has to be done offline by reconstructing the tracks from the drift chambers and determine a possible kink in the track which gives the interaction point and the scattering angle. We estimated a number of about 2.5×10^5 useful scattering event to be detected during the planned measurements. Useful in the sense that they are in the t-range from -0.002 to -0.007. A rough estimate of the accuracy for an asymmetry measurement $\delta\epsilon$ with N events is calculated by $\delta\epsilon = \sqrt{(\frac{\delta\epsilon}{\delta L})^2 + (\frac{\delta\epsilon}{\delta R})^2}$ with $L = R = N/4$ for the events on the left (L) and right (R) side used to calculate $\epsilon = \frac{L-R}{L+R}$. With 20% polarization *i.e.* $\epsilon = P \times A_y = 0.009$ and 2.5×10^5 events an error $\delta\epsilon$ of $\sim 30\%$ results which is consistent to MC studies resulting in an asymmetry of $\epsilon = 0.012 \pm 24\%$ based on 2.5×10^5 events.

4. Summary

The polarization study of produced antiprotons will clarify the question if the antiproton production process creates some polarization. If so, it would be the ideal basis for the preparation a polarized antiproton beam.

The described detector setup was installed at the T11 beam line at CERN and a first measurement was successfully completed in December 2014. Preliminary analyses confirm the expected online pion discrimination and a clear antiproton separation in the offline reconstruction. The detailed data analysis will begin in 2015.

REFERENCES

[1] A.D. Krisch, *AIP Conf. Proc.* **145**, 11 (1986).

[2] E. Steffens, *AIP Conf. Proc.* **1008**, 1 (2008).

[3] E. Steffens, *AIP Conf. Proc.* **1149**, 80 (2009).

[4] H.-O. Meyer, *AIP Conf. Proc.* **1008**, 124 (2008).

[5] K.A. Olive *et al.* [Particle Data Group], *Chin. Phys.* **C38**, 090001 (2014).

[6] A. Bravar *et al.*, *Phys. Rev. Lett.* **77**, 2626 (1996).

[7] P.L. Csonka, *Nucl. Instrum. Methods* **63**, 247 (1968).

[8] K. Kilian, Symp. on HEP with polarized beams and targets, Lausanne 1980, Birkhäuser Verlag, pp. 219–227, 1981.

[9] K. Kilian, D. Möhl, Proceedings, Physics at LEAR, Erice, CERN/PS/LEA, pp. 701–710, 1982.

[10] F. Rathmann *et al.*, *Phys. Rev. Lett.* **71**, 1379 (1993).

[11] J.M. Richard, Symp. on HEP with polarized beams and targets, Lausanne 1980, Birkhäuser Verlag, pp. 535–540, 1981.

[12] C. Barschel *et al.* [PAX Collaboration], `arXiv:0904.2325 [nucl-ex]`.

[13] V.F. Dmitriev, A.I. Milstein, S.G. Strakhovenko, *Nucl. Instrum. Methods* **B266**, 1122 (2008).

[14] V.F. Dmitriev, A.I. Milstein, S.G. Salnikov, *Phys. Lett.* **B690**, 427 (2010).

[15] P. Lenisa, F. Rathmann for the PAX Collaboration, `arXiv:hep-ex/0505054`.

[16] D. Oellers *et al.*, *Phys. Lett.* **B674**, 269 (2009).

[17] W. Augustyniak *et al.*, *Phys. Lett.* **B718**, 64 (2012).

[18] B. Schoch, *Eur. Phys. J.* **A43**, 5 (2010).

[19] K. Kilian *et al.*, *Int. J. Mod. Phys.* **A26**, 757 (2011).

[20] E.J. Ramberg, *Phys. Lett.* **B338**, 403 (1994).

[21] B.Z. Kopeliovich, L.I. Lapidus, *Sov. J. Nucl. Phys.* **19**, 114 (1974).

[22] N.H. Buttimore *et al.*, *Phys. Rev.* **D59**, 114010 (1999).

[23] D.P. Grosnick *et al.*, *Nucl. Instrum. Methods* **A290**, 269 (1990).

[24] N. Akchurin *et al.*, *Phys. Rev.* **D48**, 3026 (1993).

[25] H. Okada *et al.*, *Phys. Lett.* **B638**, 450 (2006).

[26] N. Akchurin *et al.*, *Phys. Lett.* **B229**, 299 (1989).

[27] J. Haidenbauer, private communication.

[28] J. Haidenbauer, G. Krein, *Phys. Rev.* **D89**, 114003 (2014).

[29] `http://sba.web.cern.ch/sba/Documentations/Eastdocs/docs/T11_Guide.pdf`

[30] T. Eichten *et al.*, *Nucl. Phys.* **B44**, 333 (1972).

[31] S. Brauksiepe *et al.*, *Nucl. Instrum. Methods* **A376**, 397 (1996).

[32] J. Smyrski *et al.*, *Nucl. Instrum. Methods* **A541**, 574 (2005).

[33] T.A. Armstrong *et al.*, *Phys. Lett.* **B385**, 479 (1996).

[34] A. Zink *et al.*, *JINST* **B9**, C04014 (2014).